Supporting information for:

Environmental Chemicals Modulate Polar Bear (*Ursus maritimus*) Peroxisome Proliferator-Activated Receptor Gamma (PPARG) and Adipogenesis *in Vitro*

*Heli Routti *,†, Roger Lille-Langøy ‡, Mari K. Berg †,‡, Trine Fink §, Mikael Harju ||, Kurt Kristiansen ⊥, Pawel Rostkowski ⫞, Marte Rusten ‡,▽, Ingebrigt Sylte ⊥, Lene Øygarden †,‡, Anders Goksøyr ‡*

† Norwegian Polar Institute, Fram Centre, 9296 Tromsø, Norway

‡ Department of Biology, University of Bergen, 5020 Bergen, Norway

§ Department of Health Science and Technology, Aalborg University, 9220 Aalborg, Denmark

|| Norwegian Institute for Air Research, Fram Centre, 9296 Tromsø, Norway

⊥ Department of Medical Biology, Faculty of Health Sciences, UiT - The Arctic University of Norway, 9037 Tromsø, Norway

⫞ Norwegian Institute for Air Research, 2007 Kjeller, Norway

Number of pages: 40

Number of tables: 6

Number of figures: 8

Preparation of polar bear tissue extracts

Contaminants were extracted from polar bear liver and adipose tissue from a healthy 10-year-old male bear (258 kg) obtained from the Governor of Svalbard (the bear was shot in self-defense July 2010 in Svalbard, Norway). Samples were wrapped in aluminum foil and stored at -20°C until further analysis. The liver (68 g) and adipose tissue (12 g) were homogenized in dry Na_2SO_4 (Emsure®, ACS, ISO, Reag. Ph Eur, purchased from Merck, KGaA, Darmstadt, Germany) and packed into columns for extraction with acetone/cyclohexane (1/3 v/v and 1/1 v/v, respectively). All solvents n-hexane, cyclohexane, acetone, dichloromethane and methanol were purchased from Merck (Suprasolv, ≥99.8%). The samples were cleaned by adding the lipid extracts onto a 30 cm long semipermeable membrane device (SPMD), a lay flat, low density polyethylene tubing (Environmental Sampling Technologies, Inc. MO, USA) and collecting the extracts. This removed 88% and ~98% of lipid from the liver and adipose tissue, respectively. Further cleanup was achieved using a high performance liquid chromatography (HPLC) system utilizing gel permeation chromatography, to remove remaining lipids from the samples. A final cleanup step was performed using a column packed with activated Florisil (0.150-0.250 mm, Merck), fractionating the sample into three fractions. The first fraction contained neutral compounds such as PCBs, PBDEs and organochlorine pesticides, while the second and third fraction contained $MeSO_2$-PCBs/DDE and hydroxylated (OH) PCBs/phenols, respectively.

The second fraction was later cleaned of lipid residues using a column with 25% sulfuric acid silica. The third fraction was cleaned by liquid-liquid extraction using 1 M potassium hydroxide in 50% ethanol (Aq) and *n*-hexane. The basic extract was acidified using 2 M HCl and back-extracted to a mixture of cyclohexane/tertbutyl methyl ether (9/1 v/v). Finally, the concentrated extract was cleaned using liquid-liquid extraction with concentrated sulphuric acid. All the extracts were evaporated to 0.5 ml (*n*-hexane or cyclohexane) using a Turbovap 500 (Biotage AB, Sweden),

transferred to 2 ml vials (conical bottom) and further evaporated using nitrogen gas, giving a final volume of 50 µl. Dimethyl sulphoxide (DMSO, BioReagent, ≥99.9%, Sigma-Aldrich Norway AS) was added and the samples were mixed by vortex and put in an ultrasonic bath for 20 min. The samples were further evaporated of any residual solvent using nitrogen gas until the weight was constant. The volume of DMSO was adjusted until the concentrations of the extracts were equivalent to 100 times the concentrations measured in polar bear tissues.

A subsequent adipose tissue extract was prepared as described above using 23 g polar bear adipose tissue. This extract was used for exposing polar bear adipose tissue-derived stem cells.

Quantification of POPs in extracts

To quantify the contaminants in the extracts, the equivalent of 6 g of the liver sample and 1 g of the adipose tissue were added ^{13}C standards of PCBs, PBDEs, organochlorine pesticides, OH-PCBs, pentachlorophenol (PCP), and a surrogate standard for the $MeSO_2$-PCBs. Standard-spiked samples were then extracted and cleaned-up parallel to the main samples above. Fraction 3, containing OH-PCBs and PCP, was further derivatized using derivatization reagent N-nitroso-N-methylurea (purchased from Angene International) before a final cleanup on a SPE-column with 25% sulfuric acid silica. Analysis of PCBs, PBDEs, DDT and its derivates, and organochlorine pesticides, OH-PCBs, PCP and $MeSO_2$-PCB/DDE was performed using GC/MS as previously described.[1,2] Average recoveries (%) ± standard deviation of ^{13}C-labeled standards in liver and adipose tissue for was 53 ± 3.3 for 14 PCBs, 63 ± 16 for four PBDEs, 62 ± 14 for six chlordanes, 79 ± 18 for three hexachlorocyclohexanes, 193 ± 95 for hexachlorobenzene, 63 ± 2.5 for mirex, 48 ± 0.7 for *p,p'*-DDE, and 47 ± 3.5 for surrogated standard $3MeSO_4$-MePCB 120. Recoveries for phenolic compounds was below 1% and for *p,p'*-DDT below 3%.

Preparation of synthetic mixtures

Three separate synthetic mixtures including 44 neutral POPs, 10 neutral POPs, and 16 $MeSO_2$-metabolites of POPs were composed according to the concentrations and composition found in polar bear adipose tissue (Table S1). The mixture of 10 neutral POPs contained only compounds present at more than 0.1µM in the 44 neutral POP mixture. The mixtures were all prepared by mixing synthetic standards dissolved in DMSO. Standards were purchased from LGC Standards (Sweden), Cambridge Isotope Laboratories (Andover, Massachusetts, USA), Greyhound Chromatography and Allied Chemicals (Birkenhead, Merseyside, United Kingdom) and Sigma-Aldrich (St. Louis, MO, USA). $MeSO_2$-PCBs/DDE was kindly donated by Centers for Disease Control and Prevention (Atlanta, USA).

Suspect/Non-target screening

Extracts of liver and adipose tissue were prepared for suspect/non-target screening as described above with the following modifications: 5 g of liver and 3 g of polar bear adipose tissue were homogenized in dry Na_2SO_4, packed in columns and added an internal standard of 50 ng of ^{13}C hexabromocyclododecane and 5 ng of the surrogate standard $MeSO_2$-4Me-PCB120. The procedure followed the method described above, but the final extracts were solved in acetonitrile instead of DMSO. The adipose tissue and liver extracts were analysed using an Agilent 1290 ultra-high performance liquid chromatography (UHPLC) system with an Accucore Polar column (250 mm x 2.1 mm, 2.6 µm; Thermo Scientific) coupled with Agilent 6550 high resolution quadrupole time-of-flight (HR-QTOF) mass spectrometer with Dual Jet Stream electrospray source operating in the positive and negative mode. The mobile phases in positive ionization mode (PI) were (A) MeOH with 5 mM ammonium formate and 0.01% v/v HCOOH and (B) an aqueous solution with 5% of MeOH, 5 mM ammonium formate and 0.01% HCOOH. For negative ionization mode (NI), the

mobile phases were (A) MeOH with 5 mM ammonium acetate and (B) an aqueous solution with 5% of methanol and 5 mM ammonium acetate. The detector operated in the range of 25-1700 Da, with gas temperature 200 °C, drying gas 18l/min, nebulizer 30 psig, sheath gas temperature 300°C and sheath gas flow 12 l/min. To ensure maximum sensitivity of the method for compounds on the list of suspects, all samples were initially analyzed in a full scan mass spectrometry (MS) mode. The samples were then reanalyzed in a MS/MS mode with different collision energies to facilitate sufficient confirmation of the compounds from the suspect list and tentative identification of unknown compounds.

Identification, cloning and sequencing of two distinct isoforms of polar bear PPARG

For pbPPARG2, a biopsy of adipose tissue was collected from an adult male polar bear in April 2011 at Svalbard as a part of the yearly monitoring programme of the Norwegian Polar Institute. The bear was immobilized by Zoletil® 100 (Virbac, France) and the adipose tissue sample was collected using a sterile 8 mm biopsy bunch, transferred to a mRNAse free cryovial, frozen immediately in liquid nitrogen and stored in -80°C until further analyses. For pbPPARG1, a piece of polar bear liver, obtained from the native subsistence hunts from Canadian Arctic, was kindly provided by R. J. Letcher (Environment Canada, National Wildlife Research Centre, Carleton University, Ottawa, Canada).

Total RNA was extracted from adipose tissue RNA using the TRIzol® Reagent (Invitrogen, Carlsbad, CA, USA) according to the suppliers' protocol. cDNA was synthesized using Superscript II reverse transcriptase and oligo$(dT)_{12\text{-}18}$ primers (both from Invitrogen) according to the manufacturer's instructions. Total RNA of the liver sample was further enriched with regards to poly A mRNA using the Dynabeads® mRNA purification kit (Life Technologies, Carlsbad, CA, USA) following the manufacturers' instructions.

A partial gene fragment of pbPPARG was amplified by gradient PCR using primers designed on the basis of the dog PPARG sequence (NM_001024632) (Table S2) and GoTaq® DNA Polymerase (Promega, Madison, WI, USA). 5´ and 3´-end pbPPARG sequences were obtained by SMARTer™ RACE cDNA amplification kit (Clonetech, Mountain View, CA, USA) using gene specific primers (Table S2). The sequence of polar bear PPARG was confirmed by sequencing.

Luciferase reporter assay (LRA)

To construct an LRA plasmid encoding a fusion protein of the GAL4 DNA-binding domain (DBD) and the hinge and ligand-binding domain (LBD) of pbPPARG2, the gene region encoding amino acids 205-505 of pbPPARG, cloned from polar bear adipose tissue, was amplified using Takara Ex Taq® DNA polymerase (Clontech) and primers introducing EcoRI and BamHI sites in the amplicons (Table S2). The pbPPARG LBD amplicon was inserted between EcoRI and BamHI sites of the pCMX-GAL4 vector,[3] constructing the plasmid pCMX-GAL4-pbPPARG. The pCMX-GAL4 vector, as well as other LRA plasmids; the tk-(MH100)x4-luciferase reporter plasmids and pCMV-β-galactosidase control plasmids, were gifts from Bruce Blumberg (University of California, Irvine). LRA was performed in COS7 cells, that unless otherwise specified, were cultivated in Dulbecco′s Modified Eagle′s Medium (DMEM) supplemented with 10% foetal bovine serum (FBS), 4 mM L-glutamine, 2 mM sodium pyruvate, and 100 U/mL penicillin-streptomycin (all from Sigma Aldrich) at 37˚C and 5% CO_2. To initiate the LRA, 5000 COS7 cells were seeded per well in 96-well plates and cultivated for 24 hours before they were transiently co-transfected with pCMX-GAL4-pbPPARG, tk(MH100)x4-luciferase, and pCMV-β-galactosidase at a mass ratio of 1:2:2 using the TransIT®-LT1 Transfection Reagent (Mirus Bio, Madison, WI, USA) as described by the manufacturer. 24 hours later, the transfected cells were exposed to test chemicals diluted in exposure medium (phenol red-free DMEM [Invitrogen, Oslo, Norway] supplemented

with 10% resin and charcoal stripped FBS, 4 mM L-glutamine, 2 mM sodium pyruvate and 100 U/mL penicillin-streptomycin) for 24 hours. After exposure, the cells were lysed, and enzymatic activity was measured as previously described.[4] Test compounds for agonistic effects included the polybrominated diphenyl ethers BDE28, BDE47, BDE99, BDE100, and BDE153, hexabromocyclododecane (HBCDD), bisphenol A (BPA), tetrabromobisphenol A (TBBPA), PCB118, PCB138, PCB153, PCB170, *p,p'*-DDE, and endosulfan. We assessed antagonistic effects of BPA, HBCDD, PCB-153, p,p'-DDE, oxychlordane, and endosulfan by exposing the cells to the test compounds in the presence of 0.5 μM of a known PPARG ligand, rosiglitazone (Cayman Chemical, Tallinn, Estonia). Antagonistic effects were tested for compounds of different structures that showed very low or no agonistic effects. The PBDEs and HBCDD were kindly donated by Åke Bergman, the University of Stockholm. PCB118 was acquired from LGC Standards (Teddington, UK) and PCB153 from ChemService (West Chester, PA, USA). The remaining compounds were obtained from Sigma-Aldrich (Oslo, Norway). We also tested agonistic and antagonistic effects of the mixture of neutral POPs, and the mixture of $MeSO_2$-metabolites of POPs. Each measurement was performed in triplicates and repeated at least three times, except agonistic effects of mixtures, which were repeated only twice.

Modeling of PPARG-ligand interactions

Polar bear PPARG ligand binding potential of environmental contaminants was studied using protein-ligand docking and scoring methods. As pbPPARG and human PPARG (hPPARG) LBD amino acid identities are 100% (Figure S2), 3D X-ray structures of hPPARG were used for docking into the LBD of pbPPARG. Five 3D X-ray crystal structures of hPPARG (1.5-2.3 Å) in complex with ligands (PBD: 3u9q, 3et3, 1zgy, 2hwq, 3b1m; Table S3) were selected among fifteen X-ray crystal structures available (PDB.org). The selection of crystal structures in

complex with a structurally diverse set of ligands was made using a cluster tree analyses using the software Internal Coordinate Mechanics (ICM) version 3.5.

A molecular mechanical approach was used to calculate the potential for receptor binding of the test compounds to h/pbPPARG LBD. First, potential binding sites in the LBD were searched for using ICM Pocket Finder.[5,6] Docking of the receptor by ligands in the X-ray crystal structure complexes was done using the Monte Carlo global optimization method. The docking predicted different binding poses of the test compound in the LBD of the model. During docking, the target structure was rigid, whereas the test compound was flexible. A diverse set of test compound poses was generated in the test compound-PPARG docking. The virtual ligand screening (VLS) scoring function was used to predict binding of test compounds to PPARG, and compared and evaluated relative to data achieved for the ligands in the X-ray crystal structures. Using the VLS scoring function in ICM, binding poses of test compounds were ranked based on their docking scores. VLS scores for the ligands bound in the crystal structures of PPARG ranged from -34.21 to -36.00 (Table S3). Test compounds with VLS scores below -31 were considered as compounds with high putative binding affinities towards pbPPARG.

3T3-L1 differentiation assay

Murine 3T3-L1 preadipocytes (ATCC-CL-173), purchased from LGC standards (Borås, Sweden) or donated by Jørn Sagen (Haukeland University Hospital), were maintained in cultivation medium (Dulbecco′s Modified Eagle′s Medium [DMEM] with 4500 mg/l glucose supplemented with 100 U/ml penicillin-streptomycin solution, 4 mM L-glutamine, 1 mM sodium pyruvate [all from Sigma Aldrich] and 10% calf serum [PAA Laboratories/GE Healthcare, Copenhagen, Denmark or Sigma Aldrich) at 37˚C and 5% CO_2. During cultivation of the preadipocytes, cell density was kept below 70-80% confluency and at passage number six or lower.

To study how extracts and synthetic mixtures affect adipogenesis in 3T3-L1 cells through the first wave of the differentiation process,[7] adipogenesis was carried out without the first-wave adipogenic mixture (isobutylmethylxanthine [IBMX], dexamethazone [DEX], and insulin). The cells were seeded in 96-well plates at a density of 960 cells/well (3000 cells/cm^2) 2 days preceding the experiment (day -2). At day 0 the medium was exchanged for culture medium (DMEM - high glucose, 100 U/ml penicillin-streptomycin, 4 mM L-glutamine, 1 mM sodium pyruvate, 10% FBS [PAA Laboratories/GE Healthcare, Copenhagen, Denmark]) and added insulin as well as the contaminant extracts, synthetic mixtures, or controls. Effect of contaminant extracts from polar bear adipose tissue and liver, including neutral POPs, MeSO2-POPs, and their combination were tested. The synthetic mixtures included 44 neutral POPs, $MeSO_2$-POPs, as well as a combination of these two mixtures. The culture medium, including insulin and test extracts/synthetic mixtures/controls, was renewed every 2-3 days. Contaminant extracts and synthetic mixtures dissolved in DMSO were diluted 1:100 (v/v) to DMEM to give a final concentration of contaminants in the DMEM equivalent to the concentrations found in polar bear tissues, and a solvent concentration of 1% (v/v). To investigate a dose-response effect, the contaminant mixtures were further diluted 1:3, 1:9, and 1:27. The DMSO/solvent used for negative control in experiments with extracts was subjected to the same extraction steps as the extracts of polar bear tissues. Rosiglitazone (1 µM in DMSO) was used as positive control. For our maximum induction control, the culture medium given at day 0 contained 1 µg/ml insulin, 1 µM rosiglitazone, 500 µM IBMX and 1000 nM DEX (all from Sigma Aldrich). The culture medium given the following days only contained added insulin (1 µg/ml). At day 10, the content of triglycerides in the 3T3-L1 cells was quantified spectrophotometrically (OD_{570nm}, Adipogenesis Detection Kit Abcam, Cambridge, UK). The experiment was repeated three times on single wells (without intra-assay replicates).

Cytotoxicity was assessed by measuring the amount of lactate dehydrogenase released into the culture medium using Cytotoxicity Detection Kit Plus (LDH; Roche, Oslo, Norway).

Further, we studied the effect of synthetic mixtures on terminal differentiation, a process primarily driven by PPARG.[7] Cells were seeded to 6-well plates and cultivated in cultivation medium until confluent (day -2). Two days later (day 0), the first wave of adipogenesis was initiated by changing the medium to culture medium (DMEM - high glucose, 100 U/ml penicillin-streptomycin, 4 mM L-glutamine, 1 mM sodium pyruvate, 10% FBS) supplemented with adipogenic cocktail (500 µM IBMX, 250 nM DEX and 5 µg/ml insulin). Terminal differentiation was initiated at day 2, when the media was changed to culture medium added 5 µg/ml insulin and the test compounds or control (rosiglitazone). At day 4, the media was exchanged for culture medium, which was subsequently renewed every other day for four days. The tested contaminant mixtures included synthetic mixtures of 44 neutral POPs and $MeSO_2$-POPs. Synthetic mixtures dissolved in DMSO were diluted 1:100 (v/v) in DMEM to give a final concentration of contaminants equivalent to concentrations in polar bear tissues, and a solvent concentration of 1% (v/v). To study dose-response relationships, the mixtures were further diluted 1:2 and 1:10. In the differentiation control, cells were exposed to rosiglitazone at a final concentration of 2 µM, and DMSO (1% v/v) was used as undifferentiated control. At day 10 the cells were fixed and triglycerides and cholesteryl oleate were stained with Oil Red O (ORO) according to methods previously described.[8] ORO was eluted with 100% isopropanol and quantified spectrophotometrically ($OD_{500\ nm}$). The exposures were performed in triplicates and each experiment was repeated three times.

Isolation and growth of polar bear adipose tissue-derived stem cells (pbASCs)

Subcutaneous adipose tissue was collected from a male and a female polar bear (10 and 7 years old, respectively) from Svalbard in September 2012. The bears were immobilized by Zoletil ® 100 (Virbac, France) and the adipose tissue samples were obtained using an 8 mm sterile biopsy punch. Biopsies were placed in phosphate buffered saline (PBS) and kept at room temperature. Stem cells were isolated from the adipose tissue as previously described [9] within 48 hours of harvest. Cells in passage 2 were frozen in aliquots of 1 x 10^6 cells and stored in vapor phase of liquid nitrogen.

Thawed polar bear adipose tissue-derived stem cells (pbASCs) were resuspended in culture medium (α-MEM supplemented with 10 % FBS, 100 U/ml penicillin-streptomycin solution, 4 mM L-glutamine, 0.05 mg/ml gentamicin). Residual freezing medium was removed by centrifugation (500 x g for 5 minutes), before the cells were resuspended in fresh culture medium and seeded at a density of 3000 cells/cm^2 in 300 cm^3 cell culture flasks. Cells were cultured at 37°C and 5% CO_2, and medium replaced twice a week. At approximately 70% confluency, the cells were subcultured. The cells were washed twice with PBS and detached from the culture flasks using 0.125% trypsin/0.01% EDTA (Sigma-Aldrich) (3 min, 37˚C) and reseeded at 3000 cells/cm^2. Cell density was determined using a haemocytometer and viability was evaluated using trypan blue (BioWhittaker™).

Cells at passage 4 were cryogenically frozen. The cells were distributed in aliquots of approximately 1 x 10^6 cells in cold freezing medium (consisting of culture medium supplemented with 30% FBS, 10% DMSO) (Sigma-Aldrich), frozen at -80 ºC for 24 hours and transferred to the vapor phase of nitrogen. All subsequent experiments were performed on cells in passage 5. The low passage number was used to avoid variation in cell shape and size between experiments, as time spent in culture affected the morphology of the cells. The cultured pbASCs grew in an adherent monolayer (Figure S5). The cells were all thin, small, and spindle-shaped and uniform in

shape in early passages (Figure S5A). As cells reached higher passages, the morphology of some of the cells changed into wider, larger and triangular-shaped cells (Figure S5B). Cells of either morphology appeared to dominate separate areas of the plate. The larger cells grew slower than the smaller cells. These observations are in accordance with several other studies [10-13].

Establishment of a method to study adipogenesis by contaminants in polar bear adipose tissue-derived stem cells (pbASCs)

As pbASCs had not previously been studied, to our knowledge, suitable conditions for adipogenic differentiation needed to be established. Seven adipogenic media consisting of culture medium supplemented with different adipogenic inducing compounds, such as IBMX, indomethacin (INDO) (Sigma-Aldrich), DEX and rosiglitazone (ROSI) (Table S4), were tested to find a medium which led to adipogenic differentiation of the pbASCs. Non-induced control cells were maintained in basal medium (culture medium supplemented with 1 µg/mL insulin and 0.1 % (v/v) DMSO). The cells were seeded at a density of 20,000 cells/cm^3 in 6-well plates and cultured to 100 % confluency (day -2). After two days cells were given adipogenic media, which was changed day 3, 7 and 10, and cultured for 14 days. The experiment was conducted once, in triplicates.

Adipogenic differentiation was measured as an increase in lipids (mainly triglycerides). This was conducted by staining the cells with Oil Red O (ORO) and subsequently eluting ORO from the cells for spectrophotometric quantification, as described by Ramirez- Zacarias *et al*. [8]. The cells were fixed *in situ* in 10 % formalin (Sigma-Aldrich) at 4°C for a minimum of 1 hour while protected from light, and subsequently washed twice with PBS and incubated with ORO working solution (freshly prepared; 3 parts 0.35 % (w/v) ORO (Sigma-Aldrich) in isopropanol (Kemetyl),

2 parts deionized water, filtered before use) for 15 minutes. The cells were washed repeatedly with deionized water until the washing solution was clear. Following washing, excess water was removed, and plates were left to dry. ORO was eluted from the cells by from the cells by addition of 100 % isopropanol. After 10 minutes of incubation the isopropanol was carefully collected. The absorbance of eluates was measured at 500 nm wavelengths, in triplicates.

Visual inspection of ORO stained cells revealed that all sample wells with cells that received adipogenic media contained cells which had accumulated lipids in vacuoles, to varying extents. No lipid accumulation was observed in wells containing non-induced control cells (Figure S6). Cell death was observed in all wells which received media containing 200 µM INDO (MII200, MDII200 and MDII200R; Figure S6B), indicating that 200 µM INDO might be toxic for pbASCs. Cells which received media containing 50 µM INDO (MII50, MDII50, and MDII50R) showed less signs of distress, and lipid content measured by eluted ORO from the cells were significantly higher ($p<0.01$) than in non-induced control cells. Cells receiving IBMX, DEX, and ROSI, but no INDO (MDI+ROSI), had the highest lipid content with an approximate three-fold increase in lipid content compared to control cells (Figure S6B; $p <0.01$). Comparable lipid content was observed in cells receiving MDII50R-medium, while the lipid content in cells cultured in MDII50- and MII50-medium was approximately twice as high as in the control cells (Figure S6B, $p<0.01$). As the medium containing MDI+ROSI led to the highest accumulation of the media tested, it was used as a positive control in subsequent experiments.

The effect of ROSI on the adipogenic differentiation of pbASCs was investigated by inducing cells in MDI, MDI+ROSI (Table S4) in the presence of 0.1 % DMSO (v/v) for two weeks. Non-induced control cells were maintained in basal medium supplemented with 0.1 % DMSO. The experiment was conducted once, in duplicates. The lipid content in cells induced by MDI

medium was twice the amount as in the non-induced control cells ($p<0.01$), indicating that MDI medium induces adipocyte differentiation of pbASCs (Figure S6C). The lipid content in cells receiving MDI+ROSI was three times higher than in cells induced by MDI ($p<0.05$), indicating that 1 µM ROSI strongly induces adipogenic differentiation in pbASCs. Based on these findings we decided to use MDI-medium as the differentiated control with a low level of differentiation, to allow for discrimination of effects of test chemicals on adipogenic induction in future experiments.

Transcript levels of adipocyte specific genes during different stages of adipogenic differentiation

Relative transcript levels of *PPARG*, fatty acid binding protein 4 (*FABP4*) and leptin (*LEP*) were studied during different stages of adipogenic differentiation in pbASCs. RNA was extracted from pbASCs cultured in BM, MDI medium, or MDI with 1 µM ROSI, in the presence of 0.1% DMSO, for 2, 6, 10 and 14 days. Adipogenic differentiation of pbASCs was performed in 12-well plates and otherwise conducted as described above. RNA was isolated from pbASCs according to the manufacturer's instructions (Aurum Total RNA mini kit, Bio-Rad, Oslo, Norway). cDNA was synthetized using the iScript™ cDNA synthesis kit (Bio-Rad, Oslo, Norway) according to the supplier's instructions. Transcript levels of target genes *PPARG*, *FABP4*, *LEP* and reference genes tyrosine 3/tryptophan 5-monooxygenase activation protein (*YWHAZ*) and cyclophilin A (*PPIA*), were determined using a LightCycler® 480 System (Roche, Basel, Switzerland). Primer sequences obtained by nucleotide BLAST in a polar bear genome sequence assembly (Ursus_maritimus.scaf.fa.gz) and estimated annealing temperatures are shown in Table S5. The reactions were carried out in triplicates using the iQ™ SYBR® Green Supermix (Bio-Rad, Oslo, Norway) in total reaction volumes of 20 µL (300 nmol of primers, 5 µL of cDNA diluted 1:10).

The real-time qPCR thermal cycling included an initial 3 minute step at 95ºC, followed by 30 cycles of 10 seconds at 95ºC for DNA denaturation, 30 seconds at the annealing temperature of the primers (Table S5), and 30 seconds at 72ºC for elongation. Product specificity was confirmed by a melting curve analysis after each assay. The relative expression of the tested genes was calculated on the basis of standard curves derived from serial dilutions of linearized plasmids (pSC-A, Agilent Technologies) containing the selected gene sequences. The transcript levels were first normalized against each reference genes. A geometric mean of the two normalized values were used for further fold change calculations.

The stability of the reference genes was evaluated by variance in the CT values for all *YWHAZ* and *PPIA* samples originating from the experiment where the gene expression of selected target genes during adipogenic differentiation were investigated (n=23, one sample was omitted as no CT value was obtained for that sample) using RefFinder. RefFinder uses software from four of the most common methods used to evaluate gene stability, including Genorm, NormFinder, and BestKeeper. All methods showed similar results. The results from BestKeeper were as follows: Mean of CT of *YWHAZ* samples was 20.35, with a standard deviation of 0.26, while the mean CT and standard deviation for *PPIA* samples were 18.78 and 0.19. The Pearson correlation coefficients and P-values were 0.857 and 0.001 for *YWHAZ* samples, and 0.730 and 0.001 for *PPIA* samples, respectively. These results indicate that the reference genes were stable across experimental conditions and thus suitable reference genes for studying adipogenesis in pbASCs.

As *PPARG* and *FABP4* transcript levels were induced by MDI and MDI+ROSI throughout the induction period (Figure S7), these genes were used ad markers for adipogenic differentiation in subsequent experiments.

Testing effects of endocrine disrupting chemicals on adipogenic differentiation in pbASCs

pbASCs were exposed to two known endocrine disruptors; mono(2-ethylhexyl)phthalate **(**MEHP) and bisphenol A (BPA) in the presence of 0.1% DMSO, supplemented in BM or MDI medium for 14 days. Cells were stained with ORO to quantify lipid content, and mRNA expression was studied by real-time Q-PCR in parallel experiments. Cells from the same culture flasks were used, as well as the same media batch, to provide conditions as similar as possible. All three MEHP exposures (BM+50 μM, MDI+10 μM and MDI+50 μM) resulted in higher lipid content and transcript levels of *PPARG* and *FABP4*, compared to non-exposed control cells (undiff. and DMSO) (Figure S8). Cells exposed to 10 and 50 μM BPA in MDI-medium had a lower lipid content compared to non-induced control cells. The cells exposed to 50 μM BPA in MDI-medium also had lower *PPARG* transcript levels compared to the control. No change in lipid content was measured in cells exposed to 50 μM BPA in BM, but a slight increase in the transcript level of *PPARG* was detected. Exposure to BPA did not result in change of transcription levels of *FABP4*.

Table S1. Concentrations (nM) of (a) neutral, (b) $MeSO_2$, and (c) OH-compounds in the synthetic mixtures and extracts from polar bears tissues. LOD: limit of detection.

a)

	Synthetic mixture	Adipose tissue extract	Liver tissue extract
Compound	nM	nM	nM
Hexachlorobenzene	49.41	49.41	24.44
α-hexachlorocyclohexane	2.26	2.26	1.46
β-hexachlorocyclohexane	49.79	49.79	43.51
γ-hexachlorocyclohexane		<LOD	0.03
Heptachlor		<LOD	<LOD
Heptachlor epoxide	330.65	330.65	-
Oxychlordane	1833.08	1833.08	160.51
trans-chlordane		<LOD	<LOD
cis-chlordane	1.21	1.21	0.24
trans-nonachlor	13.10	13.10	19.67
cis-nonachlor	0.25	<LOD	0.25
Mirex	30.11	30.11	2.60
o.p'-DDE		-	-
p.p'-DDE	36.48	36.48	0.94
o.p'-DDD		-	-
p.p'-DDD	1.45	1.45	-
o.p'-DDT		-	-
p.p'-DDT	2.24	2.24	-
PCB 18	2.39	<LOD	<LOD
PCB 28/31	3.41	0.18	0.10
PCB 33		0.07	0.02
PCB 47/49		3.91	4.14
PCB 52	7.22	0.16	0.09
PCB 66		0.11	0.20
PCB 74	0.60	4.22	2.99
PCB 99	137.85	140.12	149.95
PCB 101	79.87	0.24	0.82
PCB 105	0.81	5.03	5.93
PCB 114/122		0.72	0.85
PCB 118	12.91	18.52	25.32
PCB 123		<LOD	0.22
PCB 128	9.73	3.05	3.93
PCB 138	113.60	87.84	113.60
PCB 141	59.84	<LOD	<LOD
PCB 149	191.19	<LOD	0.32
PCB 153	1136.11	1136.65	1169.29

PCB 156	74.82	74.32	79.59
PCB 157	4.14	62.33	67.29
PCB 167	3.65	0.83	1.22
PCB 170	657.70	662.31	568.24
PCB 180	1037.13	1022.86	784.41
PCB 183	48.85	12.03	7.65
PCB 187	102.15	4.02	3.75
PCB 189	2.22	67.67	74.10
PCB 194	826.02	835.10	696.52
PBDE 17	0.01	<LOD	<LOD
PBDE 28	0.05	<LOD	<LOD
PBDE 49		<LOD	<LOD
PBDE 47	15.31	15.31	1.14
PBDE 66	0.09	<LOD	<LOD
PBDE 71		<LOD	<LOD
PBDE 77		<LOD	<LOD
PBDE 100	2.42	<LOD	<LOD
PBDE 119		<LOD	<LOD
PBDE 99	12.46	<LOD	<LOD
PBDE 85	0.57	<LOD	<LOD
PBDE 154	0.78	<LOD	<LOD
PBDE 153	1.22	8.29	<LOD
PBDE 138	0.13	<LOD	<LOD
SUM	6895.26	6510.87	4009.90

b)

Compound	Synthetic mixture nM	Adipose tissue extract nM	Liver tissue extract nM
3-$MeSO_2$-PCB52		<LOD	<LOD
3-$MeSO_2$-PCB49	41.73	42.57	11.57
4-$MeSO_2$-PCB52		<LOD	<LOD
4-$MeSO_2$-PCB49	42.57	19.51	<LOD
3-$MeSO2_2$-PCB91	0.00	141.85	19.89
4-$MeSO_2$-PCB91	19.51	129.58	17.79
3-$MeSO_2$-PCB101	141.85	1.92	17.20
4-$MeSO_2$-PCB101	129.58	77.74	34.47
3-$MeSO_2$-DDE	1.92	<LOD	<LOD
3-$MeSO_2$-PCB87	77.74	18.64	2.63
3-$MeSO_2$-PCB110	0.00	6.15	4.95
4-$MeSO_2$-PCB110	18.64	47.10	5.41
3-$MeSO_2$-PCB149	6.15	0.41	0.90
4-$MeSO_2$-PCB149	47.10	20.89	2.93
3-$MeSO_2$-PCB132	0.41	18.65	3.49
4-$MeSO_2$-PCB132	20.89	16.10	1.89
3-$MeSO_2$-PCB141	18.65	1.25	2.93
4-$MeSO_2$-PCB141	16.10	2.18	<LOD
3-$MeSO_2$-PCB174	1.25	<LOD	<LOD
4-$MeSO_2$-PCB174	2.18	<LOD	<LOD
SUM	586.27	544.54	126.05

c)

Compound	Synthetic mixtures nM	Adipose tissue extract nM	Liver tissue extract nM
Pentachlorophenol	45.05	7.51	0.65
4-OH-HpCS	8.11	1.35	0.69
4-OH-PCB 120		<LOD	<LOD
4-OH-PCB 107	150.41	25.07	1.39
3-OH-PCB 153		-	2.96
4-OH-PCB 146	56.21	9.37	0.98
3-OH-PCB 138		<LOD	0.52
4-OH-PCB 130		<LOD	<LOD
4-OH-PCB 163		<LOD	0.33
4-OH-PCB 187	274.70	45.78	0.60
4-OH-PCB 172	70.72	11.79	0.30
4'-OH-PCB 193	136.51	22.75	0.53
2-OH-BDE68		<LOD	-
6-OH-BDE47/75		<LOD	-
5-OH-BDE47		<LOD	-
4-OH-BDE49		<LOD	-
5-OH-BDE100		<LOD	-
4-OH-BDE103		<LOD	-
TBBPA		-	-
5-OH-BDE99		<LOD	-
4-OH-BDE101		<LOD	-
SUM	741.72	123.62	8.95

Table S2. Primer sequences used for cloning and identification of polar bear PPARG from adipose (PPARG2) and liver tissue (PPARG1).

Primer	Sequence (5'-3')	Area of use
PPARG_F	TGACATCAAGCCATTCACCACCG	Amplification of initial pbPPARG segment, fwd
PPARG_R	CAAGGACGCCAGCATCGTGT	Amplification of initial pbPPARG segment, rev
MT97	CAATTGGAAAAAGGAACACG	Amplification of full-length pbPPARG, rev
MT476	GGTATCAACGCAGAGTACG	Amplification of full-length pbPPARG, fwd
MT633	GTTTCTTGAATTCCATAATGCCATCAGGTTTGG	Amplification of h/pbPPARG-LBD, fwd; EcoRI
MT624	GTTTCTTGGATCCCTAGTACAAGTCCTTGTAGATC	Amplification of h/pbPPARG-LBD, rev; BamHI
MT80	ATTCAATTGCCATGAGGGAGTTGGAAGG	5´-RACE gene-specific primer (GSP), pbPPARG2
MT81	ATGCAGGCTCCACTTTGATTGCACTTTG	5´-RACE GSP, pbPPARG1
MT82	CATTCGCATCTTTCAGGGGTGTCAGTTC	3´-RACE GSP, pbPPARG

Table S3. PPARG X-ray crystal structures and docking score of ligands bound to the ligand binding domain in these structures.

X-ray crystal structure	Known ligand	Chemical structure	Score
3u9q	dka[a]	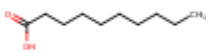	-34,6
3et3	et[b]	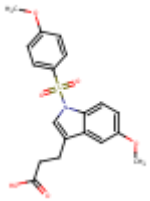	-36
1zgy	brl[c]	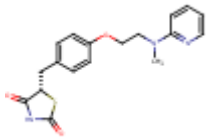	-32,46
2hwq	dry[d]	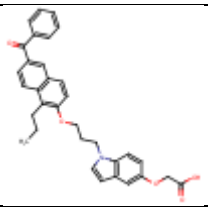	-34,21
3b1m	krc[e]	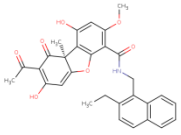	-34,16

[a] Decanoic acid

[b] 3-{5-methoxy-1-[(4-methoxyphenyl)sulfonyl]-1H-indol-3-yl}propanoic acid

[c] 2,4-Thiazolidinedione, 5-[[4-[2-(Methyl-2-Pyridinylamino)Ethoxy]Phenyl]Methyl]-(9cl)

[d] [(1-{3-[(6-Benzoyl-1-Propyl-2-Naphthyl)Oxy]Propyl}-1h-Indol-5-Yl)Oxy]Acetic Acid

[e] (9aS)-8-acetyl-N-[(2-ethylnaphthalen-1-yl)methyl]-1,7-dihydroxy-3-methoxy-9a-methyl-9-oxo-9,9a-dihydrodibenzo[b,d]furan-4-carboxamide

Table S4. Concentration of adipogenic inducers in tested adipogenic media. IBMX: 3-isobutyl-1-methylxanthine; INDO: indomethacin; DEX; dexamethasone; ROSI: rosiglitazone

Media	IBMX (μM)	Insulin (μg/mL)	INDO (μM)	DEX (μM)	ROSI (μM)
Basal medium (BM) /control		1			
MII200	450	1	200		
MDII200	450	1	200	0.1	
MDII200R	450	1	200	0.1	1
MII50	450	1	50		
MDII50	450	1	50	0.1	
MDII50R	450	1	50	0.1	1
MDI	450	1		0.1	
MDI+ROSI	450	1		0.1	1

Table S5. Primers used for amplification of target and reference genes in polar bear adipose tissue-derived stem cells.

Name	Direction	Sequence (5'-3')	Annealing Temperature (ºC)	Primer efficiency
PPARG	Forward	CACAATGGCATCAGGTTTGG	57	1.95
	Reverse	GGGGGTGATGTGGTGTTTGAAC		
FABP4	Forward	GAAGTAGGAGTGGGCTTTGC	57	1.86
	Reverse	AGGACACCTCCATCTAAGGTT		
YWHAZ	Forward	ACTTTTGGTACATTGTGGCTTCAC	60	1.88
	Reverse	CCGCCAGGACAAACCAATAT		
PPIA	Forward	GTCTCCTTTGAGCTGTTTGC	57	1.89
	Reverse	AGTCTTGGCAGTGCAGATGA		

Table S6. Compounds detected by suspect/non-target analyses.

CAS	name	formula	confidence
Adipose tissue extract (all fractions)			
1506-02-1	tonalide	C18H26O	1
29679-58-1	fenoprofen	C15H14O3	3
54739-30-9	13-OxoODE ((9Z,11E)-13-Oxooctadeca-9,11-dienoic acid)	C18H30O3	2
2315-61-9	4-Octylphenol di-ethoxylate	C18H30O3	3
117-84-0	Di-n-octylphthalate (DOP)	C24H38O4	1
6422-86-2	bis(2-ethylhexyl)terephthalate	C24H38O4	1
4651-67-6	3-α-hydroxy-7-oxo-5-β-cholan-24-oic acid	C24H38O4	3
117-81-7	DEHP (Bis(2-ethylhexyl) phthalate)	C24H38O4	1
84-74-2 / 84-69-5	dibutyl or diisobutyl phthalate	C16H22O4	2
26761-40-0	diisodecyl phthalate	C28H46O4	2
84-76-4	dinonyl phthalate	C26H42O4	2
28553-12-0	diisononyl phthalate	C26H42O4	2
	cis-9, trans-11, trans-13-conjugated linolenic acid		
Liver neutral extract (fraction 1)			
	3b-hydroxy-5-cholenoic acid	C24H38O3	2
148-82-3	melphalan	C13H18Cl2N2O2	3
23202-81-5	methyl 5-deoxy-2,3-O-isopropylidene-ß-D-ribofuranoside	C9H16O4	3
53445-37-7	2,2,4(or 2,4,4)-trimethyladipic acid	C9H16O4	3
123-99-9	azelaic acid	C9H16O4	3
1636-27-7	dipropylmalonic acid	C9H16O4	3
924-88-9	diisopropyl succinate	C10H18O4	3
111-20-6	sebacic acid	C10H18O4	3
2425-79-8	1,4-bis(2,3-epoxypropoxy)butane	C10H18O4	3
1137-42-4	4-Hydroxybenzophenone	C13H10O2	3
117-99-7	2-Hydroxybenzophenone	C13H10O2	3
90-46-0	xanthydrol	C13H10O2	3
39515-51-0	m-phenoxybenzaldehyde	C13H10O2	3
1852-04-6	undecanedioic acid	C11H20O4	2
	4,7-dimethyl-3a,4,5,6,7,7a-hexahydro-1H-inden-1-yl propanoate	C14H22O2	3
50650-75-4	4-methyl-6-(2,4,4-trimethylpentyl)-2H-pyran-2-one	C14H22O2	3
1139-46-4	4-(2,4,4-Trimethyl-2-pentanyl)-1,2-benzenediol	C14H22O2	3
5888-33-5	exo-1,7,7-trimethylbicyclo[2.2.1]hept-2-yl acrylate	C13H20O2	3
35836-72-7	(1R,5S)-2-(6,6-dimethylbicyclo[3.1.1]hept-2-en-2-yl) ethyl acetate	C13H20O2	3
3457-61-2	tert-butyl α,α-dimethylbenzyl peroxide	C13H20O2	3
15458-48-7	1,2,3,6,-tetrahydro-N-(2-hydroxyethyl)phthalimide	C10H13NO3	3
658-48-0	methyrosine	C10H13NO3	3
3467-59-2	N-(2,5-dimethoxyphenyl)acetamide	C10H13NO3	3

	2-butyloctyl-sulfonic acid	C12H26O4S	3
4706-78-9	dodecyl sulfuric acid	C12H26O4S	3
27830-12-2	2-(octyloxy)benzoic acid	C15H22O3	3
25812-30-0	Gemfibrozil	C15H22O3	3
118-60-5	2-ethylhexyl salicylate	C15H22O3	3
	2-(2-dodecyloxyethoxy)ethyl sulfonic acid	C16H34O6S	3
125-51-9	pipenzolate	C22H28NO3	3
3811-75-4	Hexamidine	C20H26N4O2	3
4754-44-3	tetradecyl sulfate	C14H30O4S	3
25157-64-6	2,4,6(1H,3H,5H)-Pyrimidinetrione, 5,5'-(1,2-diazenediyl)bis-	C8H6N6O6	3
14009-24-6	drotaverin	C24H31NO4	3
7695-91-2	Tocopherolacetate	C31H52O3	2
828-00-2	2,6-dimethyl-1,3-dioxan-4-yl acetate	C8H14O4	3
32167-31-0	Hydroxyethylated 2-butyne-1,4-diol	C8H14O4	3
3437-84-1	bisisobutyryl peroxide	C8H14O4	3
6413-10-1	ethyl 2-methyl-1,3-dioxolane-2-acetate	C8H14O4	3
627-93-0	dimethyl adipate	C8H14O4	3
1117-31-3	1,3-butylene diacetate	C8H14O4	3
42031-28-7	trans-2-isopropyl-5-carboxy-1,3-dioxane	C8H14O4	3
12772-98-4	debacterol	H2O4S	3
90-30-2	N-phenyl-1-naphthylamine	C16H13N	3
17865-07-5	propyltriacetoxysilane	C9H16O6Si	3
31566-31-1	stearic acid, monoester with glycerol	C21H42O4	2
30614-22-3	pirimicarb desmethyl	C10H16N4O2	3
501-68-8	Beclamid	C10H12ClNO	3
147-94-4	cytarabine	C9H13N3O5	3
84-74-2 or 84-69-5	dibutyl or diisobutyl phthalate	C16H22O4	3
26761-40-0	diisodecyl phthalate	C28H46O4	2
84-76-4	dinonyl phthalate	C26H42O4	2
28553-12-0	diisononyl phthalate	C26H42O5	2
85-68-7	butyl benzene phthalate	C19H20O4	2
104-40-5	4-nonylphenol	C15H24O	2

Liver MeSO2-extract (fraction 2)

29679-58-1	fenoprofen	C15H14O3	3
27975-19-5	isosteviol	C20H30O3	2
92-62-6	Acridine-3,6-diamine	C13H11N3	2
147441-56-3	N-Oxide-Tramadol	C16H25NO3	3
54-32-0	moxisylyte	C16H25NO3	3
1182822-31-6	Carbonic acid, 5-amino-2,4-bis(1,1-dimethylethyl)phenyl methyl este	C16H25NO3	3
303-53-7	cyclobenzaprine	C20H21N	3
109-54-6	3-chloropropyldimethylammonium	C5H12ClN	3
468-61-1	oxeladin	C20H33NO3	3
642-72-8	benzydamine	C19H23N3O	3

34432-92-3	N-ethyl-N-[2-[1-(2-methylpropoxy)ethoxy]ethyl]-4-(phenylazo)aniline	C22H31N3O2	3
3737-09-5	disopyramide	C21H29N3O	3
54644-39-2	1-ethyl-1-methylpiperidin-1-ium	C8H18N	3
13424-56-1	nicotinoylprocaine	C19H23N3O3	3
82304-66-3	7,9-Di-tert-butyl-1-oxaspiro(4,5)deca-6,9-diene-2,8-dione	C17H24O3	3
456-59-7	cyclandelate	C17H24O3	3
147613-95-4	N,N-di-n-butyl-2-(1,2-dihydro-3-hydroxy-6-isopropyl-2-quinolylidene)-1,3-dioxoindan-5-carboxamide	C30H34N2O4	3
2948-46-1	2,2'-(1,4-Phenylene)di(2-propanol)	C12H18O2	3
	Degradation-Product	C12H18O2	3
1999-85-5	α,α,α',α'-tetramethyl-m-xylene-α,α'-diol	C12H18O2	3
136-77-6	hexylresorcinol	C12H18O2	3
84-74-2 / 84-69-5	dibutyl or diisobutyl phthalate	C16H22O4	2
84-66-2	diethyl phthalate	C12H14O4	

Liver neutral, MeSO2 and OH-extract (fraction 1-3)

90-30-2	N-phenyl-1-naphthylamine	C16H13N	2
4698-11-7	10-methoxy-5H-dibenz[b,f]azepine	C15H13NO	3
86-84-0	1-naphthyl isocyanate	C11H7NO	3
130-00-7	benz[cd]indol-2(1H)-one	C11H7NO	3
104098-48-8	Imazapic	C14H17N3O3	3
59-99-4	neostigmine	C12H19N2O2	3
60207-90-1	propiconazole	C15H17Cl2N3O2	3
24589-78-4	N-Methyl-N-(trimethylsilyl)trifluoroacetamide	C6H12F3NOSi	3
832088-68-3	4-(4-(4-(hydroxydiphenylmethyl)-1-piperidinyl)-1-butynyl)-α,α-dimethylbenzeneacetic acid	C32H35NO3	3
52602-39-8	9H-carbazol-4-ol	C12H9NO	3
	Degradation-Product	C19H23NO2	3
161798-03-4	5-Thiazolecarboxylic acid, 2-[3-formyl-4-(2-methylpropoxy)phenyl]-4-methyl-, ethyl ester	C18H21NO4S	3
13669-70-0	nefopam	C17H19NO	3
83799-24-0	fexofenadine	C32H39NO4	3
82-98-4	piperidolate	C21H25NO2	3
1225-56-5	Nordoxepin	C18H19NO	3
812-70-4	2H,2H,3H,3H-perfluorodecanoic acid	C10H5F15O2	3
17243-39-9	benzoctamine	C18H19N	3
	AMX penicilloic acid	C16H21N3O6S	3
3575-80-2	metylperon	C16H22FNO	3
30223-74-6	2-ethyl-5-methyl-3,3-diphenylpyraline	C19H21N	3
438-60-8	protriptyline	C19H21N	3
72-69-5	nortriptyline	C19H21N	3
17692-39-6	fomocaine	C20H25NO2	3
65928-58-7	Dienogest	C20H25NO2	3
64-95-9	adiphenine	C20H25NO2	3

303-53-7	cyclobenzaprine	C20H21N	3
1668-19-5	curatin, lindo, doxepin, doxepinbiomo, stada, doxepin, quitaxon, doxepin teva, doxepin rph, espadox, doxepin hcl, prudoxin	C19H21NO	3
116256-11-2	1-(3-(4-fluorophenoxy)propyl)-3-methoxy-4-piperidinone	C15H20FNO3	3
147-20-6	diphenylpyraline	C19H23NO	3
125971-57-5	2-Isobutyryl-3,N-diphenylacrylamide	C19H19NO2	3
93-98-1	Benzanilide	C13H11NO	3
98243-83-5	Benalaxyl-M	C20H23NO3	3
511-45-5	Pridinol	C20H25NO	3
467-85-6	Normethadone	C20H25NO	3
	tusukal	C20H25NO	3
57808-66-9	domperidone	C22H24ClN5O2	3
90-54-0	Etafenone	C21H27NO2	3
	Degradation-Product	C21H27NO2	3
3376-94-1	norpropoxyphene	C21H27NO2	3
469-62-5	propoxyphene	C22H29NO2	3
4317-14-0	amitriptylinoxide	C20H23NO	3
86-13-5	Benztropine mesylate	C21H25NO	3
76-99-3	methadone	C21H27NO	3
2156-27-6	benproperine	C21H27NO	3
13042-18-7	fendiline	C23H25N	3
	Degradation-Product	C28H25NO4	3
524-83-4	ethybenztropine	C22H27NO	3
52602-39-8	9H-carbazol-4-ol	C12H9NO	3
1477-40-3	levacetylmethadol	C23H31NO2	3
99473-14-0	Carboxy Terbinafine	C21H23NO2	3
4658-28-0	mesoranil	C7H11N7S	3
201668-31-7	Flufenacet-OXA	C11H12FNO3	3
82-98-4	piperidolate	C21H25NO2	3
51772-35-1	N-phenyl-N-(2,4,4-trimethylpentan-2-yl)naphthalen-1-amine	C24H29N	3
3277-26-7	dimethyl[(trimethylsilyl)oxy]silyl	C5H15OSi2	3
90-69-7	Lobeline	C22H27NO2	3
17230-88-5	danazol	C22H27NO2	3
87-17-2	salicylanilide	C13H11NO2	3
91-40-7	fenamic acid	C13H11NO2	3
145599-86-6	Cerivastatin	C26H34FNO5	3
	Degradation-Product	C24H29NO2	3
4658-28-0	mesoranil	C7H11N7S	3
201668-31-7	Flufenacet-OXA	C11H12FNO3	3
	1-tetradecanoylbenzotriazole	C20H31N3O	3
6843-97-6	Dodicin	C18H39N3O2	3
93-98-1	Benzanilide	C13H11NO	3
74103-06-3	ketorolac	C15H13NO3	3
86-84-0	1-naphthyl isocyanate	C11H7NO	3

130-00-7	benz[cd]indol-2(1H)-one	C11H7NO	3
51997-51-4	9H-Carbazole, 4-(2-oxiranylmethoxy)-	C15H13NO2	3
86-84-0	1-naphthyl isocyanate	C11H7NO	3
130-00-7	benz[cd]indol-2(1H)-one	C11H7NO	3
1823-37-6	IDM KETAL	C14H11NO	3
519-87-9	diphenylacetamide	C14H13NO	3
621-06-7	phenylacetanilide	C14H13NO	3
54041-17-7	N-(4-Fluorophenyl)-2-hydroxy-N-(1-methylethyl) acetamide	C11H14FNO2	3
2920-38-9	p-phenylbenzonitrile	C13H9N	3
260-94-6	acridine	C13H9N	3
52602-39-8	9H-carbazol-4-ol	C12H9NO	3
578-95-0	Acridone	C13H9NO	3
61-68-7	mefenamic acid	C15H15NO2	3
256-96-2	Iminostilbene	C14H11N	3
93-98-1	Benzanilide	C13H11NO	3
1823-37-6	IDM KETAL	C14H11NO	3
69555-14-2	Glycine, N-(diphenylmethylene)-, ethyl ester	C17H17NO2	3
58-00-4	Apomorphine	C17H17NO2	3
	benzyl(3-hydroxyphenacyl)methylammonium c	C16H17NO2	3
14657-64-8	3-(hydroxyphenylphosphinyl)propanoic acid	C9H11O4P	3
957-51-7	Diphenamid	C16H17NO	3
27589-33-9	azosemide	C12H11ClN6O2S2	3
83891-03-6	Norfluoxetin	C16H16F3NO	3
54910-89-3	Fluoxetine	C17H18F3NO	3
27589-33-9	azosemide	C12H11ClN6O2S2	3
23465-76-1	caroverine	C22H27N3O2	3
65513-61-3	metholachlor-desmethyl	C14H20ClNO2	3
15972-60-8	alachlor	C14H20ClNO2	3
34256-82-1	acetochlor	C14H20ClNO2	3
226256-56-0	Cinacalcet	C22H22F3N	3
6195-20-6	AMIN AGK 559; cyl 3-amino-4-chlorobenzoate	C19H30ClNO2	3
23184-66-9	Butachlor	C17H26ClNO2	3
55837-29-1	tiropramide	C28H41N3O3	3
126-27-2	oxethazaine	C28H41N3O3	3
71937-28-5	1-aminoethylphosphinic acid	C2H8NO2P	3
84-74-2 or 84-69-5	dibutyl or diisobutyl phthalate	C16H22O4	3
26761-40-0	diisodecyl phthalate	C28H46O4	3
84-76-4	dinonyl phthalate	C26H42O4	2
28553-12-0	diisononyl phthalate	C26H42O5	2
85-68-7	butyl benzene phthalate	C19H20O4	2

```
ATGGGTGAAACTCTGGGAGATTCTCTTATTGACCCAGAAAGCGATTCCTTTGCTGATACACTGTCTGCAAGCACTTCACAAGAAATTACCATGGTTGACA  < 100
 M  G  E  T  L  G  D  S  L  I  D  P  E  S  D  S  F  A  D  T  L  S  A  S  T  S  Q  E  I  T  M  V  D  T
CCGAGATGCCATTTTGGCCCACCAACTTTGGAATCAGCTCCGTGGATCTCTCTGTAATGGATGACCACTCCCATTCTTTTGACATCAAGCCCTTCACCAC  < 200
  E  M  P  F  W  P  T  N  F  G  I  S  S  V  D  L  S  V  M  D  D  H  S  H  S  F  D  I  K  P  F  T  T
CGTGGATTTCTCCAGCATTTCCACTCCACACTATGAAGACATTCCATTTGCAAGAGCGGACCCAATGGTTGCTGATTACAAGTATGACCTGAAGCTCCAG  < 300
 V  D  F  S  S  I  S  T  P  H  Y  E  D  I  P  F  A  R  A  D  P  M  V  A  D  Y  K  Y  D  L  K  L  Q
GAGTACCAAAGTGCAATCAAAGTGGAGCCTGCATCCCCACCTTATTATTCGGAAAAGACTCAGCTGTACAATAAGCCTCATGAAGAGCCTTCCAACTCCC  < 400
E  Y  Q  S  A  I  K  V  E  P  A  S  P  P  Y  Y  S  E  K  T  Q  L  Y  N  K  P  H  E  E  P  S  N  S  L
TCATGGCAATTGAATGCCGAGTCTGTGGAGATAAAGCTTCCGGGTTCCACTATGGCGTTCATGCTTGTGAAGGATGCAAGGGGTTCTTCCGGAGGACAAT  < 500
  M  A  I  E  C  R  V  C  G  D  K  A  S  G  F  H  Y  G  V  H  A  C  E  G  C  K  G  F  F  R  R  T  I
CAGATTGAAGCTCATTTATGATAGGTGTGACCTTAACTGTCGGATCCATAAAAAAAGTAGAAATAAATGTCAGTACTGTCGGTTTCAGAAATGCCTTGCT  < 600
 R  L  K  L  I  Y  D  R  C  D  L  N  C  R  I  H  K  K  S  R  N  K  C  Q  Y  C  R  F  Q  K  C  L  A
GTGGGGATGTCTCACAATGCCATCAGGTTTGGGCGGATGCCGCAGGCCGAGAAGGAGAAGCTGTTGGCGGAGATCTCCAGCGATATCGACCAGCTGAACC  < 700
V  G  M  S  H  N  A  I  R  F  G  R  M  P  Q  A  E  K  E  K  L  L  A  E  I  S  S  D  I  D  Q  L  N  P
CAGAGTCGGCTGATCTCCGGGCCCTGGCAAAACATTTGTATGACTCATACATAAAGTCCTTCCCGCTGACCAAAGCAAAGGCGAGGGCGATCTTGACAGG  < 800
  E  S  A  D  L  R  A  L  A  K  H  L  Y  D  S  Y  I  K  S  F  P  L  T  K  A  K  A  R  A  I  L  T  G
AAAGACGACGGACAAATCACCATTTGTTATCTATGACATGAATTCCTTAATGATGGGAGAAGATAAAATCAAGTTCAAACACATCACCCCCTTGCAGGAG  < 900
 K  T  T  D  K  S  P  F  V  I  Y  D  M  N  S  L  M  M  G  E  D  K  I  K  F  K  H  I  T  P  L  Q  E
CAGAGCAAAGAGGTGGCCATTCGCATCTTTCAGGGGTGTCAGTTCCGCTCAGTGGAAGCTGTGCAGGAGATCACAGAGTATGCCAAAAGTATCCCTGGCT  < 1000
Q  S  K  E  V  A  I  R  I  F  Q  G  C  Q  F  R  S  V  E  A  V  Q  E  I  T  E  Y  A  K  S  I  P  G  F
TTGTAAACCTTGACTTGAATGACCAAGTAACTCTCCTAAAATATGGTGTCCATGAGATCATTTACACGATGCTGGCCTCCTTGATGAATAAAGATGGGGT  < 1100
  V  N  L  D  L  N  D  Q  V  T  L  L  K  Y  G  V  H  E  I  I  Y  T  M  L  A  S  L  M  N  K  D  G  V
TCTCATATCAGAGGGCCAAGGATTCATGACAAGGGAGTTTCTAAAGAGCCTGAGAAAGCCCTTTGGTGACTTTATGGAGCCCAAGTTTGAGTTTGCTGTG  < 1200
 L  I  S  E  G  Q  G  F  M  T  R  E  F  L  K  S  L  R  K  P  F  G  D  F  M  E  P  K  F  E  F  A  V
AAGTTCAATGCACTGGAATTAGATGACAGCGACTTGGCAATATTTATAGCCGTCATTATTCTCAGTGGAGACCGCCCAGGTTTGCTGAACGTGAAGCCCA  < 1300
K  F  N  A  L  E  L  D  D  S  D  L  A  I  F  I  A  V  I  I  L  S  G  D  R  P  G  L  L  N  V  K  P  I
TTGAGGACATCCAGGACAACCTGCTGCAAGCCTTGGAGCTCCAGCTCAAGCTGAACCACCCCGAATCCTCTCAGCTCTTTGCCAAGCTGCTCCAGAAAAT  < 1400
  E  D  I  Q  D  N  L  L  Q  A  L  E  L  Q  L  K  L  N  H  P  E  S  S  Q  L  F  A  K  L  L  Q  K  M
GACAGACCTCAGACAGATTGTAACAGAACATGTGCAGCTATTGCAAGTCATAAAGAAAACAGAGACGGACATGAGTCTTCACCCGCTCCTACAAGAGATA  < 1500
 T  D  L  R  Q  I  V  T  E  H  V  Q  L  L  Q  V  I  K  K  T  E  T  D  M  S  L  H  P  L  L  Q  E  I
TACAAGGACTTGTATTAG  < 1518
Y  K  D  L  Y  *
```

Figure S1. Nucleotide and amino acid sequence of polar bear PPARG sequences. Two pbPPARG reading frames with corresponding amino acid sequence (475 and 505 AA) were cloned. The start of the shorter isoform is highlighted by the second boxed start codon. The DNA-binding domain (DBD; former) and ligand-binding domain (LDB; latter) are underlined. PPARG-domains are based on their similarity to human (P37231) from UniProtKB [14]. The alignments were produced using Serial Cloner 2.6.1 [15].

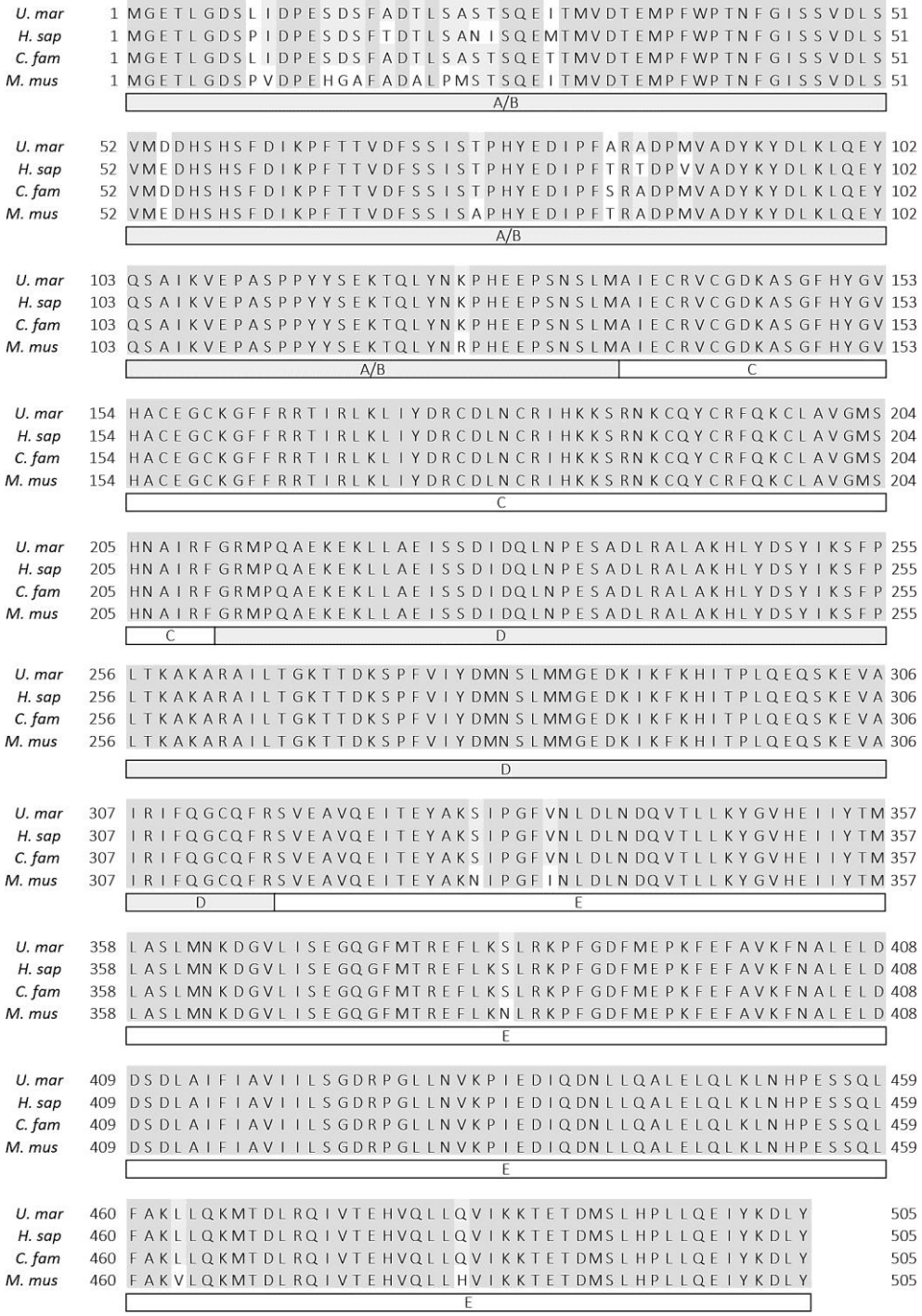

Figure S2. Multiple alignments of PPARG2 sequences. Deduced polar bear (U. mar) PPAR amino acid sequences were aligned with human (H. sap), dog (C. fam) and mouse (M. mus) amino acid sequences. The following accession numbers were used: human PPARG2 (NP_056953), dog PPARG (NP_001019803), and mouse PPARG2 (NP_035276). A/B, C, D and E-regions are indicated. UniProt identifiers used to identify receptor regions were as follows**:** P37231 (human PPARG), Q4U3Q4 (dog PPARG), and P37238 (mouse PPARG). The comparison of these PPARG orthologs confirms the high degree of conservation (100%) of the DBD (C-region) and hinge (D-region). LBD (E-region) of PPARG from human, dog, and polar bear were identical, whereas three amino acids were substituted in the LBD of mouse PPARG.

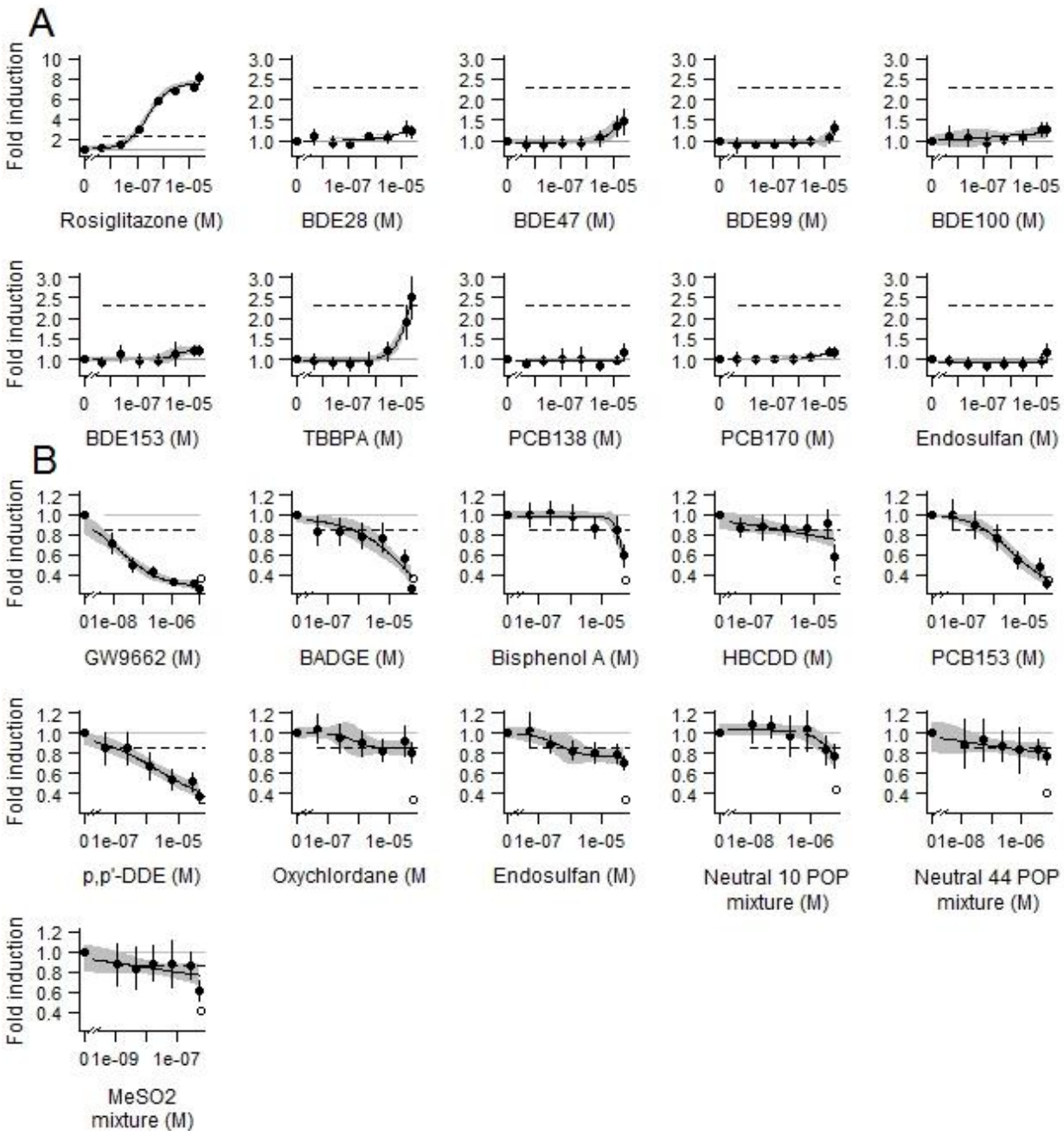

Figure S3. Agonistic (A) and antagonistic (B) luciferase activity via pbPPARG after exposure to test compounds showing significant fold induction (Table 1). COS7 cells were transiently transfected with receptor GAL4-PPARG-LBD chimeras, reporter plasmids (tk-(MH100)4-luciferase), and the constitutively active β-galactosidase plasmids (as transfection and toxicity controls). Fold induction for agonistic and antagonistic activities are expressed over control (DMSO (≤1%) for agonistic effects and 0.5 µM rosiglitazone for antagonistic effects) as average of observations (n=9-18) and 95% confidence intervals. Dose-response curves derived from log-logistic models are given with 95% confidence bands. The horizontal grey line represents luciferase activity in control-treated cells. The dashed line represents 20% of maximal effect induced by (A) rosiglitazone and (B) GW9662 in the presence of 0.5 µM rosiglitazone. Open circles (B) represent luciferase activity in cells treated only with DMSO in the absence of rosiglitazone.

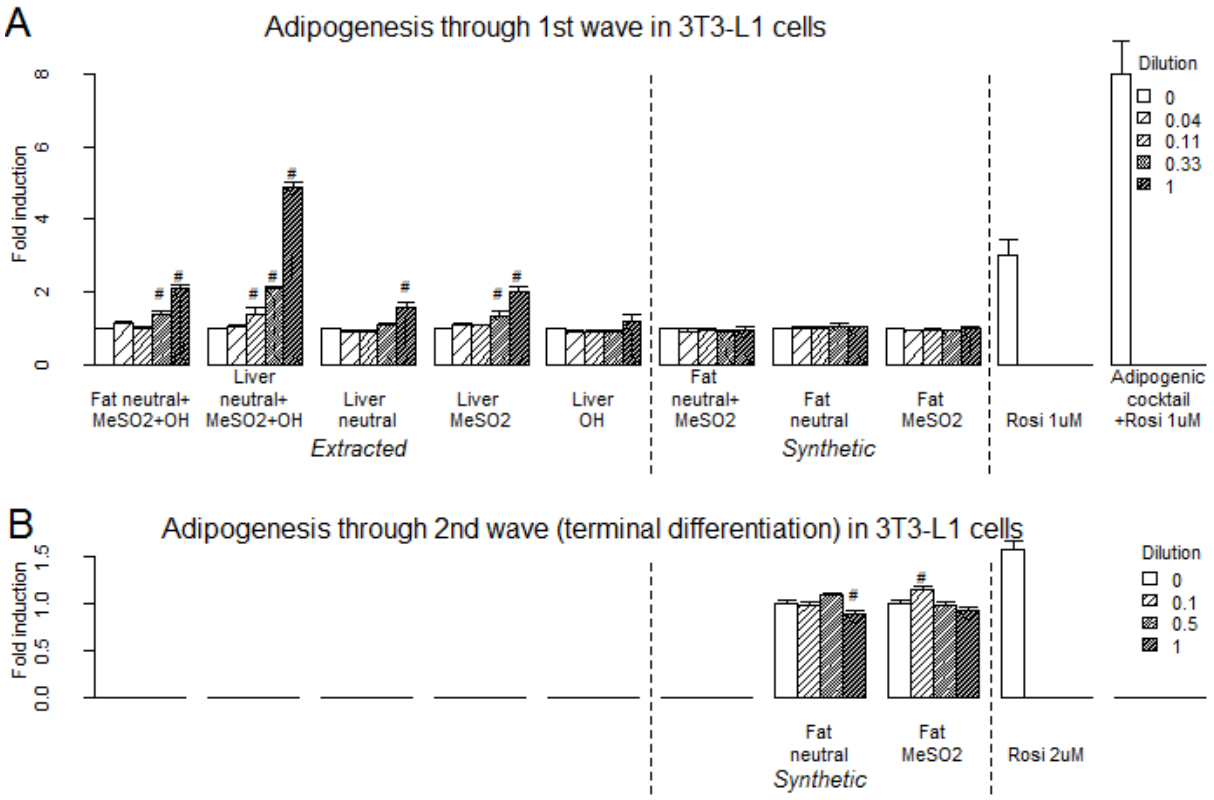

Figure S4. Effects of contaminant extracts from polar bear tissues and synthetic mixtures on triglyceride accumulation of 3T3-L1 after a 10-day growth period. Effect of tissue extracts and synthetic mixtures on differentiation of 3T3-L1 cells through the first wave (A) was determined enzymatically after exposure to culture medium including 1 µg/ml insulin and test mixtures, 1% DMSO, or rosiglitazone throughout the growth period. Adipogenic cocktail (1 µg/ml insulin, 500uM 3-isobutyl-1-methylxanthine [IBMX] and 1000nM dexamethasone [DEX]), and rosiglitazone was given to the control cells at day 0 after which they received only culture medium with 1 µg/ml insulin. Effect of synthetic mixtures of contaminants on terminal differentiation (B) of 3T3-L1 cells was determined by OilRed O staining in cells given culture medium added adipogenic cocktail (500 µM IBMX, 250 nM DEX and 5 µg/ml insulin) at day 0, culture medium added 5 µg/ml insulin and the tested mixtures (or controls) at day 2 and culture medium during days 4-10. Results are given as mean and 95% confidence intervals (CI) (n=3-9). Significant differences ($\alpha<0.05$) between test compounds and dilution 0 (DMSO) are marked with #.

A) 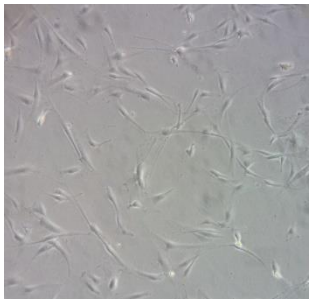 B) 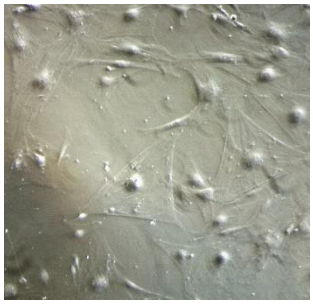

Figure S5. Cell shape and size of pbASCs. PbASCs were subcultured when approximately 70 % confluence was reached. Cells were visualized by inverted microscopy with a 10x objective. A) spindle-shaped pbASCs in passage 2. B) Triangular-shaped pbASCs in passage 7.

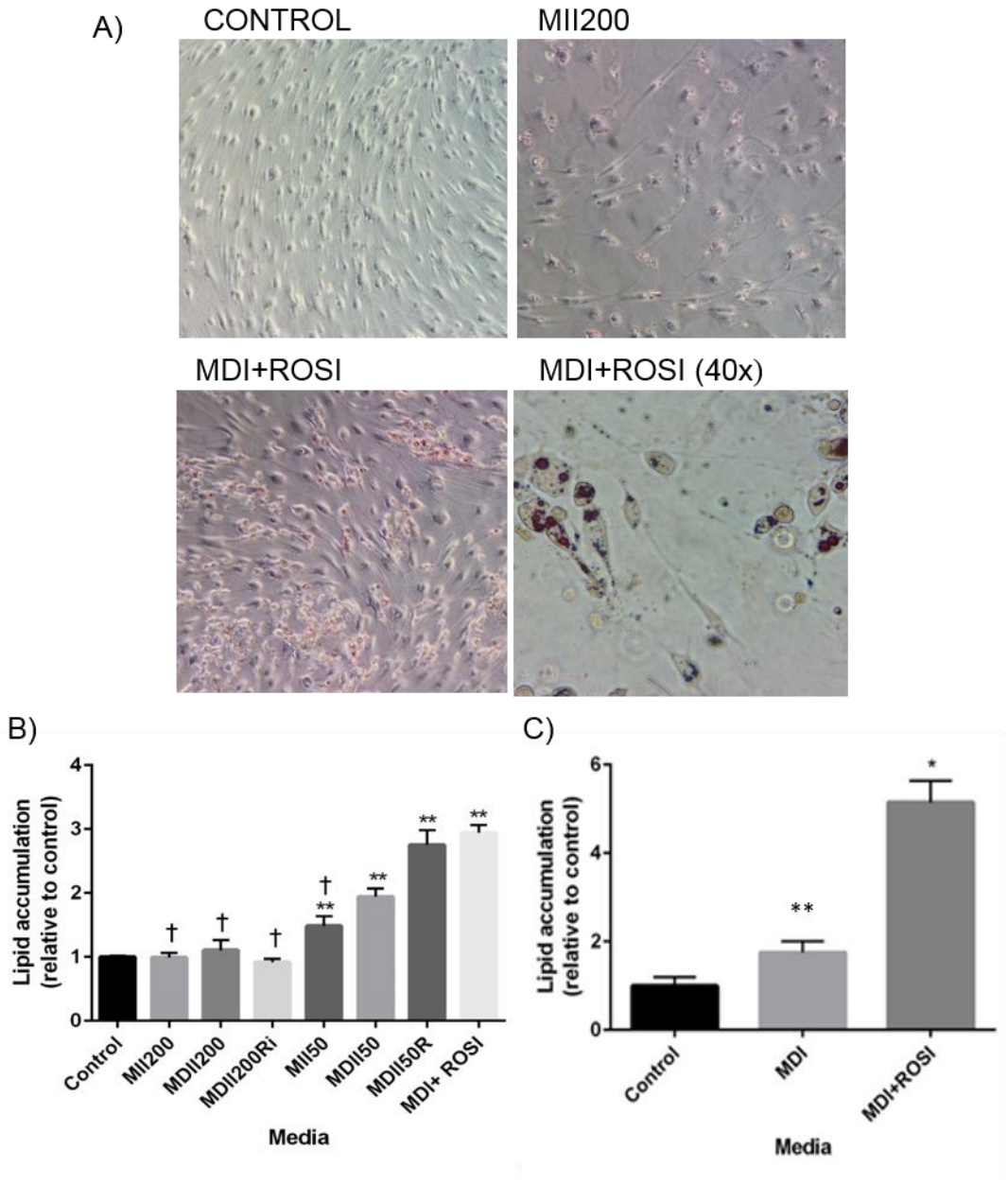

Figure S6. Effect of various adipogenic induction media (Table S4) on lipid accumulation in pbASCs cultivated for two weeks, and subsequently fixed and stained with Oil Red O (ORO). A) Cells were visualized by inverted microscopy with 10x and 40x (bottom right) objectives. The red droplets are lipids stained by ORO. B) Lipid content measured as the absorbance (λ=500 nm) in isopropanol extracts (n=3). C) Effect of rosiglitazone (1 µM) on lipid accumulation in pbASCs (n=2) was studied in the presence of 0.1% DMSO. † = high level of cell death (observed by inverted microscopy as detached cells floating in the medium and a decrease in confluence to below approximately 70 % or less during cultivation). ** = significantly different from undifferentiated control cells, α<0.01.***** = significantly different from MDI, α<0.05.

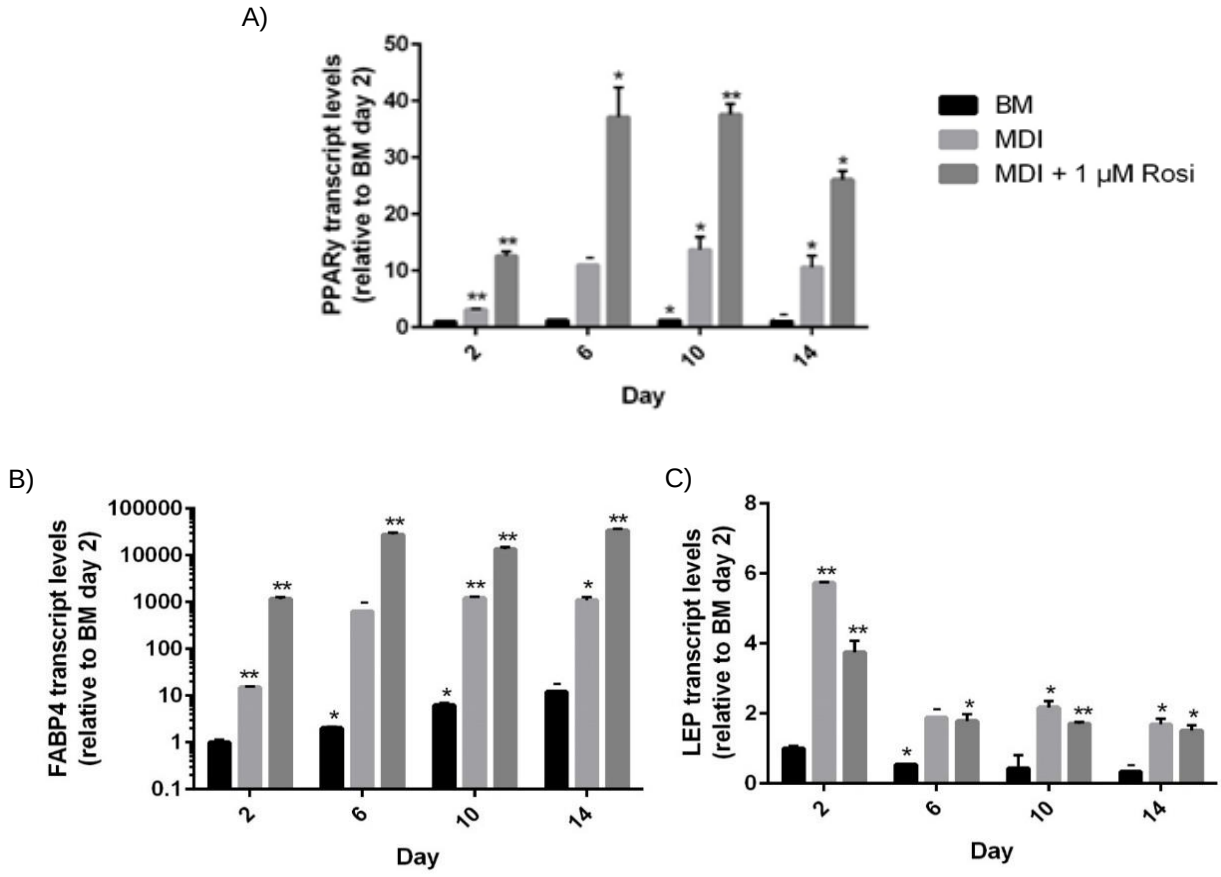

Figure S7. Relative transcript levels of *PPARG*, *FABP4* and *LEP* during different stages of adipogenic differentiation of pbASCs. RNA was extracted from pbASCs cultured in BM or MDI medium, or MDI supplied with 1 µM ROSI, in the presence of 0.1% DMSO, for 2, 6, 10 or 14 days. Following culturing, cDNA synthesis was performed and real-time Q-PCR conducted. Transcript levels were normalized against reference genes *WYHAZ* and *PPIA*, and the expression made relative to the control cells (cells cultivated in BM for 2 days). Cells were seeded in duplicates (n=2). Two samples were omitted from the analysis (MDI Day 6, and BM day 14) due to lack of a valid C_T value, or extreme aberration. * = significantly different from control cells, $\alpha<0.05$; ** = significantly different from control cells, $\alpha<0.01$.

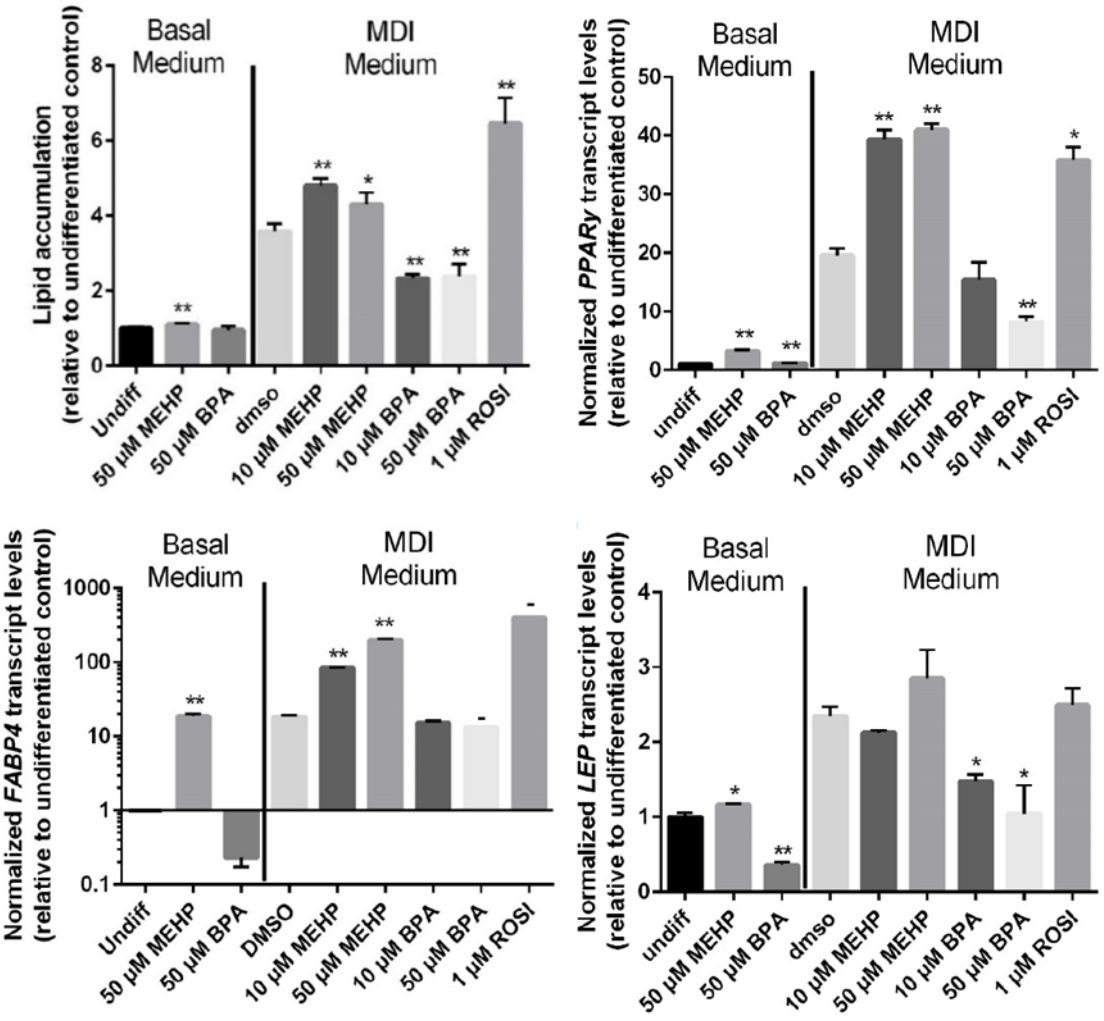

Figure S8. Effect of mono(2-ethylhexyl)phthalate (MEHP) and bisphenol A (BPA) on lipid accumulation and transcript levels of *PPARG* and *FABP4* in polar bear adipose tissue-derived stem cells (pbASCs). pbASCs were cultured for two weeks in basal medium (BM) or MDI (Table S2), supplemented with BPA, MEHP, rosiglitazone in the presence of 0.1% DMSO. Cells were stained with Oil Red O to quantify lipid content (n=3). Transcript levels of *PPARG* and *FABP4* (n=2) were normalized against reference genes (*WYHAZ* and *PPIA*) (n=2). Two samples were omitted from the FABP4 results (MDI+50 µM BPA, and MDI+1 µM ROSI) due to a lack of a valid C_T value, or extreme aberration. Results are given as mean and 95% confidence intervals over MDI supplemented with DMSO. Significant differences ($\alpha<0.05$ and <0.01) between test compounds and undifferentiated control cells are marked with * and **, respectively.

REFERENCES:

1. Sandanger, T. M.; Dumas, P.; Berger, U.; Burkow, I. C., Analysis of HO-PCBs and PCP in blood plasma from individuals with high PCB exposure living on the Chukotka Peninsula in the Russian Arctic. *J. Environ. Monit.* **2004,** *6*, (9), 758-765. doi:10.1039/b401999g

2. Nøst, T. H.; Helgason, L. B.; Harju, M.; Heimstad, E. S.; Gabrielsen, G. W.; Jenssen, B. M., Halogenated organic contaminants and their correlations with circulating thyroid hormones in developing Arctic seabirds. *Sci. Total Environ.* **2012,** *414*, 248-256. doi:10.1016/j.scitotenv.2011.11.051

3. Blumberg, B.; Sabbagh, W.; Juguilon, H.; Bolado, J.; van Meter, C.; Ong, E.; Evans, R., SXR, a novel steroid and xenobiotic-sensing nuclear receptor. *Genes Dev.* **1998,** *12*, (20), 3195-3205. doi:10.1101/gad.12.20.3195

4. Grün, F.; Venkatesan, R.; Tabb, M.; Zhou, C.; Cao, J.; Hemmati, D.; Blumberg, B., Benzoate X receptors alpha and beta are pharmacologically distinct and do not function as xenobiotic receptors. J. B*iol. Chem.* **2002,** *277*, (46), 43691-43697. doi:10.1074/jbc.M206553200

5. An, J.; Totrov, M.; Abagyan, R., Pocketome via comprehensive identification and classification of ligand binding envelopes. *Mol. Cell. Prot.* **2005,** *4*, (6), 752-761. doi:10.1074/mcp.M400159-MCP200

6. Abagyan, R.; Kufareva, I., The Flexible Pocketome Engine for Structural Chemogenomics. In *Chemogenomics: Methods and Applications*, Jacoby, E., Ed. Humana Press: Totowa, NJ, 2009; pp 249-279.

7. Lefterova, M., I.; Haakonsson, A., K.; Lazar, M., A.; Mandrup, S., PPARγ and the global map of adipogenesis and beyond. *Trends Endocrin. Metab.* **2014,** *25*, (6), 293-302. doi:10.1016/j.tem.2014.04.001

8. Ramírez-Zacarías, J. L.; Castro-Muñozledo, F.; Kuri-Harcuch, W., Quantitation of adipose conversion and triglycerides by staining intracytoplasmic lipids with oil red O. *Histochemistry* **1992,** *97*, (6), 493-497. doi:10.1007/bf00316069

9. Fink, T.; Rasmussen, J. G.; Emmersen, J.; Pilgaard, L.; Fahlman, A.; Brunberg, S.; Josefsson, J.; Arnemo, J. M.; Zachar, V.; Swenson, J. E.; Frobert, O., Adipose-derived stem cells from the brown bear (*Ursus arctos*) spontaneously undergo chondrogenic and osteogenic differentiation in vitro. *Stem Cell Res.* **2011,** *7*, (1), 89-95. doi:10.1016/j.scr.2011.03.003

10. Sekiya, I.; Larson, B. L.; Smith, J. R.; Pochampally, R.; Cui, J. G.; Prockop, D. J., Expansion of human adult stem cells from bone marrow stroma: Conditions that maximize the yields of early progenitors and evaluate their quality. *Stem Cells* **2002,** *20*, (6), 530-541. doi:10.1634/stemcells.20-6-530

11. DiGirolamo, C. M.; Stokes, D.; Colter, D.; Phinney, D. G.; Class, R.; Prockop, D. J., Propagation and senescence of human marrow stromal cells in culture: a simple colony-forming assay identifies samples with the greatest potential to propagate and differentiate. *Br. J. Haematol.* **1999,** *107*, (2), 275-281. doi:10.1046/j.1365-2141.1999.01715.x

12. Bruder, S. P.; Jaiswal, N.; Haynesworth, S. E., Growth kinetics, self-renewal, and the osteogenic potential of purified human mesenchymal stem cells during extensive subcultivation and following cryopreservation. *J. Cell. Biochem.* **1997,** *64*, (2), 278-294. doi:10.1002/(SICI)1097-4644(199702)64:2<278::AID-JCB11>3.0.CO;2-F

13. Wagner, W.; Horn, P.; Castoldi, M.; Diehlmann, A.; Bork, S.; Saffrich, R.; Benes, V.; Blake, J.; Pfister, S.; Eckstein, V.; Ho, A. D., Replicative senescence of mesenchymal stem cells: a continuous and organized process. *PloS one* **2008,** *3*, (5), e2213. doi:10.1371/journal.pone.0002213

14. UniProt Consortium, T.; Apweiler, R.; Martin, M. J.; O'Donovan, C.; Magrane, M.; Alam-Faruque, Y.; Alpi, E.; Antunes, R.; Arganiska, J.; Casanova, E. B.; Bely, B.; Bingley,

M.; Bonilla, C.; Britto, R.; Bursteinas, B.; Chan, W. M.; Chavali, G.; Cibrian-Uhalte, E.; Da Silva, A.; De Giorgi, M.; Dimmer, E.; Fazzini, F.; Gane, P.; Fedotov, A.; Castro, L. G.; Garmiri, P.; Hatton-Ellis, E.; Hieta, R.; Huntley, R.; Jacobsen, J.; Jones, R.; Legge, D.; Liu, W. D.; Luo, J.; MacDougall, A.; Mutowo, P.; Nightingale, A.; Orchard, S.; Patient, S.; Pichler, K.; Poggioli, D.; Pundir, S.; Pureza, L.; Qi, G. Y.; Rosanoff, S.; Sawford, T.; Sehra, H.; Turner, E.; Volynkin, V.; Wardell, T.; Watkins, X.; Zellner, H.; Corbett, M.; Donnelly, M.; van Rensburg, P.; Goujon, M.; McWilliam, H.; Lopez, R.; Xenarios, I.; Bougueleret, L.; Bridge, A.; Poux, S.; Redaschi, N.; Auchincloss, A.; Axelsen, K.; Bansal, P.; Baratin, D.; Binz, P. A.; Blatter, M. C.; Boeckmann, B.; Bolleman, J.; Boutet, E.; Breuza, L.; de Castro, E.; Cerutti, L.; Coudert, E.; Cuche, B.; Doche, M.; Dornevil, D.; Duvaud, S.; Estreicher, A.; Famiglietti, L.; Feuermann, M.; Gasteiger, E.; Gehant, S.; Gerritsen, V.; Gos, A.; Gruaz-Gumowski, N.; Hinz, U.; Hulo, C.; James, J.; Jungo, F.; Keller, G.; Lara, V.; Lemercier, P.; Lew, J.; Lieberherr, D.; Martin, X.; Masson, P.; Morgat, A.; Neto, T.; Paesano, S.; Pedruzzi, I.; Pilbout, S.; Pozzato, M.; Pruess, M.; Rivoire, C.; Roechert, B.; Schneider, M.; Sigrist, C.; Sonesson, K.; Staehli, S.; Stutz, A.; Sundaram, S.; Tognolli, M.; Verbregue, L.; Veuthey, A. L.; Zerara, M.; Wu, C. H.; Arighi, C. N.; Arminski, L.; Chen, C. M.; Chen, Y. X.; Huang, H. Z.; Kukreja, A.; Laiho, K.; McGarvey, P.; Natale, D. A.; Natarajan, T. G.; Roberts, N. V.; Suzek, B. E.; Vinayaka, C. R.; Wang, Q. H.; Wang, Y. Q.; Yeh, L. S.; Yerramalla, M. S.; Zhang, J.; Consortium, U., Update on activities at the Universal Protein Resource (UniProt) in 2013. *Nucleic Acids Res.* **2013,** *41*, (D1), D43-D47. doi:10.1093/Nar/Gks1068

15. Perez, F. *Serial Cloner 2.6.1*, Serialbasics: Paris, France.